Inorganic Chemistry

Forum Article

pubs.acs.org/IC

# Density Functional Theory and X-ray Analysis of the Structural Variability in $\eta^5$,$\eta^5$,$\eta^1$-Tris(ring) Rare Earth/Actinide Tetramethylpyrrolyl Complexes, $(C_5Me_5)_2M(NC_4Me_4)$

Christopher L. Webster, Jefferson E. Bates, Ming Fang, Joseph W. Ziller, Filipp Furche, and William J. Evans*

Department of Chemistry, University of California, Irvine, California 92697-2025, United States

Ⓢ *Supporting Information*

**ABSTRACT:** $(C_5Me_5)_2M(NC_4Me_4)$ complexes (M = Y, Sm, Ce, U) were synthesized to act as structural models for the $(\eta^5\text{-}C_5Me_5)_2$-$M(\eta^1\text{-}C_5Me_5)$ intermediate postulated to give pseudoalkyl reactivity to sterically crowded $(C_5Me_5)_3M$ complexes. This synthesis was accomplished through reaction of the tetraphenylborate complexes, $[(C_5Me_5)_2M][(\mu\text{-}Ph)_2BPh_2]$, with potassium tetramethylpyrrolyl, $KNC_4Me_4$. X-ray crystallographic studies on the resulting $(C_5Me_5)_2M(NC_4Me_4)$ complexes showed that, although the two $(C_5Me_5)^-$ rings bind to the metal with $\eta^5$ coordination and tetramethylpyrrolyl has a primary $\eta^1$ coordination, the complexes are not symmetrical in the solid state, and disparate M−N−C(ring) angles within a complex orient a $(NC_4Me_4)^-$ ring carbon and methyl carbon near the metal in a pseudo-$\eta^3$ binding mode. Moreover, these $(C_5Me_5)_2M(NC_4Me_4)$ complexes display unexpectedly large structural variations not only between metals but also between crystals grown from the same mother liquor. Large variations are observed in the M−N−C(ring) angles that lead to close metal ring carbon distances [105.6(1)−115.7(2)°] as well as in the M−N−($NC_4Me_4$ ring centroid) angles (152.2−167.3°). The synthesis and structure of 4d, 4f, and 5f metal examples are described, and the results are compared to predictions from the density functional theory. The reasons for the variable structures displayed by the $(C_5Me_5)_2M(NC_4Me_4)$ complexes are discussed.

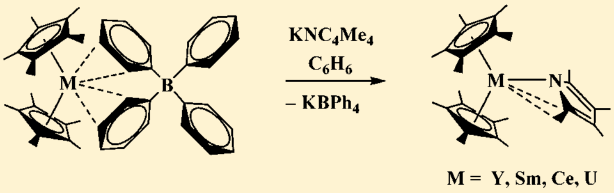

## ■ INTRODUCTION

Reactivity studies on the sterically crowded $(C_5Me_5)_3M$ complexes (M = U, La, Ce, Pr, Nd, Sm, Gd, Y) have shown that one $(C_5Me_5)^-$ ring can react as an alkyl anion even though these complexes have a tris(pentahapto) structure in the solid state.[1,2] Hence, as shown in Scheme 1, the $(C_5Me_5)_3M$ compounds can ring-open tetrahydrofuran (THF),[1] polymerize ethylene,[1] undergo hydrogenolysis,[1] and engage in $CO_2$[2] and CO[3] insertion chemistry.

This reactivity could be explained if an $\eta^1$-$C_5Me_5$ intermediate were accessible, as shown in Scheme 2, but for many years, there were no spectroscopic or structural data to support this idea. The addition of ligands to $(C_5Me_5)_3M$ complexes to force an $\eta^5$-to-$\eta^1$ conversion led to even more crowded $(C_5Me_5)_3MX$ (X = Cl, F, Me; M = U),[4,5] $(C_5Me_5)_3ML$ (L = CO,[3] and $N_2$[6] for M = U and $Me_3CCN$[7] for M = La, Ce, Pr, Nd), and $(C_5Me_5)_3LnL_2$ compounds (L = $Me_3CCN$,[7] $Me_3CNC$;[7] Ln = La−Pr), all of which maintained $\eta^5$-$C_5Me_5$ ligation in the solid state.

However, recent studies with the tetramethylcyclopentadienyl ligand $(C_5Me_4H)^-$ have provided models closer to an $\eta^5$,$\eta^5$,$\eta^1$-tris($C_5Me_5$) structure. With scandium, this ligand forms $(\eta^5\text{-}C_5Me_4H)_2Sc(\eta^1\text{-}C_5Me_4H)$[8] (Scheme 3), a complex with the $\eta^5$,$\eta^5$,$\eta^1$ structure albeit with all $(C_5Me_4H)^-$ ligands. With two $(C_5Me_5)^-$ ligands and only one $(C_5Me_4H)^-$ group, Y and Lu also form models for the $\eta^5$,$\eta^5$,$\eta^1$-tris($C_5Me_5$) structure, but these $(C_5Me_5)_2M(C_5Me_4H)$ complexes have the structure shown in Scheme 3 in which interactions with a ring carbon and methyl carbon allow them to be described as $(\eta^5\text{-}C_5Me_5)_2M(\eta^3\text{-}C_5Me_4H)$.[8]

The complexes in Scheme 3 were the first structural examples to support the possibility of $\eta^1$ intermediates in $(C_5Me_5)_3M$ chemistry. However, these examples were limited to the smallest of the rare earths: extension to the larger lanthanides proved to be complicated. In an effort to gain additional information on $\eta^5$,$\eta^5$,$\eta^1$ compounds with $(C_5Me_5)^-$, the syntheses of $[(C_5Me_5)_2M]^+$ metallocenes containing the tetramethylpyrrolyl ligand, $(NC_4Me_4)^-$ (TMN$^-$), were explored. Because TMN has an unsubstituted nitrogen atom that can function as a $\sigma$ donor, formation of an $\eta^5$,$\eta^5$,$\eta^1$ structure might be favored. Previous reports involving the rare-earth metals and uranium with monodentate pyrrolyl ligands include $^1H$ NMR spectroscopic evidence for $U(NC_4H_2Me_2)_4$,[9] as well as structural characterization of $(C_5Me_5)_2Y(\eta^1\text{-}NC_4H_4)(THF)$,[10] $(C_5H_5)_2Y(\eta^1\text{-}NC_4H_4)(THF)$,[10] and the aminobenzyl complex $(CH_2C_6H_4NMe_2\text{-}o)_2Sc(\eta^1\text{-}NC_4Me_4)$.[11] Pyrrole rings have also been used extensively with the rare earths as central components of polydentate ligands. Polydentate examples include complexes of

**Special Issue:** Inorganic Chemistry Related to Nuclear Energy

**Received:** May 3, 2012
**Published:** June 28, 2012

Scheme 1. Examples of $\eta^1$-Alkyl-Type Reactivity from $(C_5Me_5)_3M$ Complexes

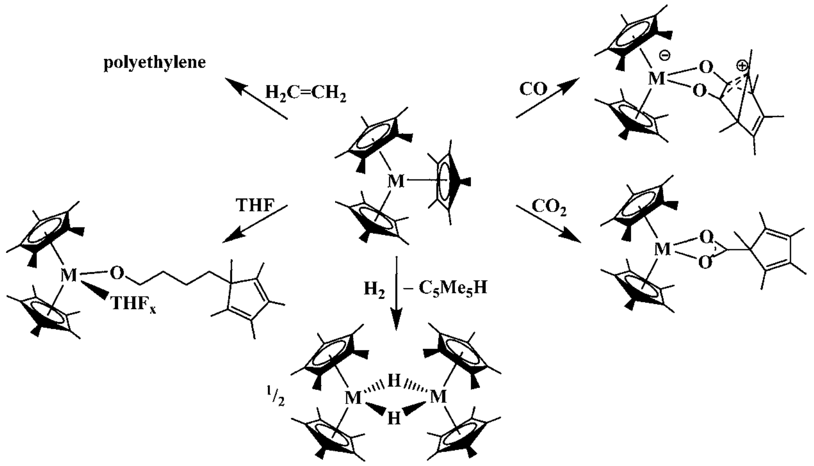

Scheme 2. Possible Formation of an $(\eta^5\text{-}C_5Me_5)_2M(\eta^1\text{-}C_5Me_5)$ Intermediate

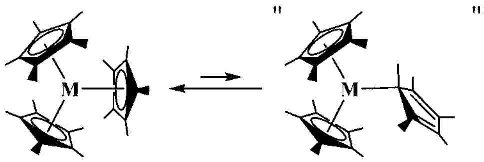

Scheme 3. Formation of $(\eta^5\text{-}C_5Me_4H)_2Sc(\eta^1\text{-}C_5Me_4H)$ and $(\eta^5\text{-}C_5Me_5)_2M(\eta^3\text{-}C_5Me_4H)$ Complexes with M = Y, Lu

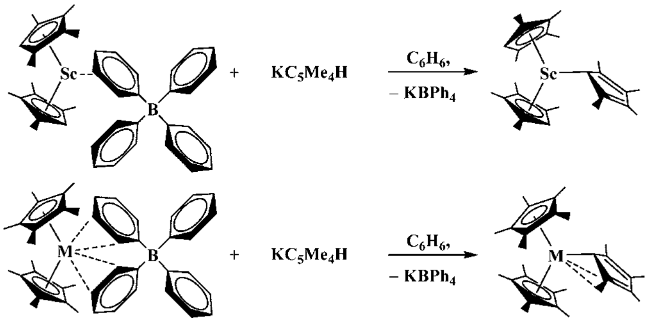

calixpyrroles,[12] Schiff base pyrroles,[12−14] binaphthyliminopyrroles,[15−17] and pyrrolylaldiminato ligands.[18] A metallocene complex of the phosphorus analogue of TMN, namely, the $(PC_4Me_4)^-$ anion ($TMP^-$), has been synthesized by Nief et al.: $(C_5Me_5)_2Sm(PC_4Me_4)$.[19] Because the nitrogen-donor atom in TMN is smaller than the phosphorus in TMP, TMN analogues of the TMP compound could have the heterocyclic ring closer to the metallocene wedge, and this would more closely mimic an $(\eta^5\text{-}C_5Me_5)_2M(\eta^1\text{-}C_5Me_5)$ intermediate. Accordingly, the synthesis of $(C_5Me_5)_2M$(TMN) compounds was pursued.

The synthetic method of choice for the $(C_5Me_5)_2M$(TMN) compounds was the reaction of $KNC_4Me_4$ with $[(C_5Me_5)_2M][(\mu\text{-}Ph)_2BPh_2]$ complexes because displacement of the weakly ligated tetraphenylborate ligand has previously been successful with a variety of alkali-metal reagents.[8,20−27] Synthetic examples with a 4d metal (Y), with 4f metals (Sm and Ce), and with a 5f metal (U) are presented along with density functional theory (DFT) analysis of the yttrium, samarium, cerium, lanthanum, and uranium homologues in this system. The order of presentation in this paper is the order of increasing principal quantum number and metal radial size according to Shannon six-coordinate radii:[28] $Y^{3+}$, $4d^0$, 0.900 Å; $Sm^{3+}$, $4f^5$, 0.958 Å; $Ce^{3+}$, $4f^1$, 1.01 Å; $U^{3+}$, $5f^3$, 1.025 Å.

## ■ EXPERIMENTAL SECTION

All syntheses and manipulations described below were conducted under argon with rigorous exclusion of air and water using glovebox, Schlenk, and vacuum-line techniques. Solvents used were dried over columns containing Q-5 and molecular sieves. NMR solvents were dried over a sodium−potassium alloy, degassed using three freeze−pump−thaw cycles, and vacuum-transferred before use. 2,3,4,5-Tetramethylpyrrole (94%) was purchased from Alfa Aesar and sublimed at room temperature to a dry ice/isopropyl alcohol (−78 °C) coldfinger under $10^{-5}$ Torr prior to use. $[(\eta^5\text{-}C_5Me_5)_2M][(\mu\text{-}Ph)_2BPh_2]$ complexes were synthesized as previously described (M = Y,[29] Sm,[30] Ce,[31] U[20]). $^1H$ NMR spectra were recorded with a Bruker DRX500 MHz spectrometer at 20 °C. IR spectra were recorded as KBr pellets on a Varian 1000 FT-IR spectrometer. Elemental analysis was performed on a Perkin-Elmer 2400 Series II CHNS analyzer.

**$KNC_4Me_4$.** This complex was made by variation of the literature method using $HNC_4Me_4$ and KH.[32] $HNC_4Me_4$ (194 mg, 1.57 mmol) was added to a stirred solution of $KN(SiMe_3)_2$ (340 mg, 1.70 mmol) in 20 mL of toluene. The clear solution turned cloudy after a few minutes. After 3 h, the slurry was centrifuged and the insoluble product was washed twice with toluene and twice with hexane to remove residual $HNC_4Me_4$ and $KN(SiMe_3)_2$ and dried in vacuo. Hydrocarbon-insoluble $KNC_4Me_4$ was dried under vacuum and isolated as a white powder (200 mg, 80%). $^1H$ NMR (THF-$d_8$, 20 °C): $\delta$ 2.00 (s, $NC_4Me_4$, 6H), 1.78 (s, $NC_4Me_4$, 6H).

**$(C_5Me_5)_2Y(NC_4Me_4)$ (YA).** Powdered $KNC_4Me_4$ (46 mg, 0.29 mmol) was added to a stirred solution of $[(C_5Me_5)_2Y][(\mu\text{-}Ph)_2BPh_2]$ (150 mg, 0.221 mmol) in 10 mL of benzene. After a few minutes, the cloudy solution turned to pale yellow and became bright yellow over 30 min. After 3 h, the solids were removed by centrifugation and filtration. Removal of the solvent from the filtrate via vacuum yielded a microcrystalline yellow solid, **YA** (106 mg, 84%). $^1H$ NMR ($C_6D_6$, 20 °C): $\delta$ 2.24 (s, $NC_4Me_4$, 6H), 1.94 (s, $NC_4Me_4$, 6H), 1.78 (s, $C_5Me_5$, 30H). Low-temperature $^1H$ NMR studies were performed from 195 to 298 K but showed no substantial change in the spectrum. Details can be found in the Supporting Information. IR: 2960s, 2907s, 2855s, 2724 m, 1516w, 1379s, 1288s, 1137s, 959s, 732s, 588m $cm^{-1}$. Anal. Calcd for $C_{28}H_{42}NY$: C, 69.84; H, 8.79; N, 2.91. Found: C, 70.19; H, 8.88, N, 2.80. Pale-yellow crystalline blocks suitable for X-ray diffraction were grown from a concentrated hexane solution at −20 °C. Two crystals were mounted on separate diffractometers in search of the best-quality data. Because the two crystals had different unit cells, crystallographic analysis was performed on each, giving two structural variations, **Y1** and **Y2**.

**$(C_5Me_5)_2Sm(NC_4Me_4)$ (Sm3).** Following the procedure for **YA** but with a 4 h reaction time, $[(C_5Me_5)_2Sm][(\mu\text{-}Ph)_2BPh_2]$ (105 mg,

Table 1. X-ray Data and Collection Parameters on Y1/Y2, Sm3, Sm-P, Ce4, and U5/U6

| | Y1 | Y2 | Sm3 | Ce4 | U5 | U6 |
|---|---|---|---|---|---|---|
| empirical formula | $C_{28}H_{42}NY$ | $C_{28}H_{42}NY$ | $C_{28}H_{42}NSm$ | $C_{28}H_{42}NCe$ | $C_{28}H_{42}NU$ | $C_{28}H_{42}NU$ |
| temperature (K) | 143(2) | 198(2) | 173(2) | 88(2) | 88(2) | 143(2) |
| cryst syst | monoclinic | monoclinic | monoclinic | monoclinic | triclinic | triclinic |
| space group | $P2_1/c$ | $P2_1/n$ | $P2_1/c$ | $P2_1/c$ | $P\bar{1}$ | $P\bar{1}$ |
| $a$ (Å) | 19.8194(10) | 12.3106(4) | 16.830(2) | 11.3214(5) | 9.2609(5) | 9.2627(6) |
| $b$ (Å) | 13.6739(8) | 13.8027(5) | 13.8251(19) | 13.9701(6) | 23.1295(13) | 16.3491(10) |
| $c$ (Å) | 22.9375(14) | 15.9133(5) | 22.983(3) | 16.8593(8) | 24.0518(14) | 17.0385(11) |
| $\alpha$ (deg) | 90 | 90 | 90 | 90 | 92.4453(7) | 88.0732(7) |
| $\beta$ (deg) | 105.3468(7) | 105.9444(4) | 105.0752(16) | 105.8122(5) | 95.9564(7) | 89.7490(7) |
| $\gamma$ (deg) | 90 | 90 | 90 | 90 | 95.5524(6) | 81.7396(7) |
| volume (Å$^3$) | 5087.2(5) | 2599.95(15) | 5163.5(12) | 2565.6(2) | 5092.8(5) | 2552.0(3) |
| $Z$ | 8 | 4 | 8 | 4 | 8 | 4 |
| $\rho_{calcd}$ (Mg m$^{-3}$) | 1.257 | 1.230 | 1.397 | 1.379 | 1.645 | 1.641 |
| $\mu$ (mm$^{-1}$) | 2.307 | 2.257 | 2.288 | 1.788 | 6.388 | 6.374 |
| R1[a] [$I > 2.0\sigma(I)$] | 0.0314 | 0.0334 | 0.0380 | 0.0185 | 0.0245 | 0.0223 |
| wR2 (all data) | 0.0776 | 0.0913 | 0.0887 | 0.0483 | 0.0587 | 0.0543 |

[a] Definitions: $R1 = \sum||F_o| - |F_c||/\sum|F_o|$; $wR2 = [\sum w(F_o^2 - F_c^2)^2/\sum w(F_o^2)^2]^{1/2}$.

0.161 mmol) and $KNC_4Me_4$ (23 mg, 0.14 mmol) yielded an orange microcrystalline solid, **Sm3** (55 mg, 73%). $^1H$ NMR ($C_6D_6$, 20 °C): $\delta$ 2.88 (s, $NC_4Me_4$, 6H), 0.38 (s, $C_5Me_5$, 30H), −11.82 (s, $NC_4Me_4$, 6H). IR: 2959s, 2913s, 2854s, 2724m, 1516w, 1378s, 1289s, 1135s, 965s, 730s, 586m cm$^{-1}$. Anal. Calcd for $C_{28}H_{42}NSm$: C, 61.93; H, 7.80; N, 2.58. Found: C, 61.40; H, 8.10, N, 2.30. Pale-orange blocks suitable for X-ray diffraction were grown from a concentrated hexane solution at −20 °C.

**($C_5Me_5$)$_2$Ce($NC_4Me_4$) (Ce4).** Following the procedure for **YA** but with a 4 h reaction time, $[(C_5Me_5)_2Ce][(\mu\text{-}Ph)_2BPh_2]$ (105 mg, 0.143 mmol) with $KNC_4Me_4$ (25 mg, 0.16 mmol) yielded a green microcrystalline solid, **Ce4** (61 mg, 80%). $^1H$ NMR ($C_6D_6$, 20 °C): $\delta$ 3.24 (s, $C_5Me_5$, 30H), 0.57 (s, $NC_4Me_4$, 6H), −31.03 (s, $NC_4Me_4$, 6H). IR: 2955s, 2905s, 2857s, 2724m, 1517w, 1378s, 1278s, 1130s, 956s, 738s, 584m cm$^{-1}$. Anal. Calcd for $C_{28}H_{42}NCe$: C, 63.12; H, 7.95; N, 2.63. Found: C, 63.40; H, 8.20, N, 2.51. Dark-green blocks suitable for X-ray diffraction were grown from a concentrated hexane solution at −20 °C.

**($C_5Me_5$)$_2$U($NC_4Me_4$) (U5).** Powdered $KNC_4Me_4$ (227 mg, 1.41 mmol) was added to a stirred solution of $[(C_5Me_5)_2U][(\mu\text{-}Ph)_2BPh_2]$ (898 mg, 1.08 mmol) in 80 mL of benzene. The brown solution turned green after 2 h. After 12 h, insoluble white solids were removed by centrifugation and filtration. The removal of solvent from the filtrate under vacuum yielded a green microcrystalline solid, **U5** (560 mg, 82%). $^1H$ NMR ($C_6D_6$, 20 °C): $\delta$ −2.62 (s, $NC_4Me_4$, 6H), −10.17 (s, $C_5Me_5$, 30H), −65.39 (s, $NC_4Me_4$, 6H). IR: 2957s, 2907s, 2854s, 2722m, 1379s, 1268s, 1134s, 1019m, 953s, 729s cm$^{-1}$. Anal. Calcd for $C_{28}H_{42}NU$: C, 53.32; H, 6.71; N, 2.22. Found: C, 53.98; H, 7.20, N, 2.66. Two structural variants were characterized by X-ray crystallography. Both were green rectangular crystals: **U5** was grown from a concentrated hexane solution at −20 °C, and **U6** was obtained from a concentrated toluene solution at −20 °C.

**X-ray Data Collection, Structure Determination, and Refinement.** Crystallographic information for complexes **Y1**, **Y2**, **Sm3**, **Ce4**, **U5**, and **U6** is summarized in Table 1 and in the Supporting Information. To check for unit cell dependence on the collection temperature, the unit cells of **Y1** and **Sm3** were measured at different temperatures in the 140−190 K range and **U5** was measured at different temperatures in the 88−140 K range. No significant change in the unit cells was observed.

**Computational Details.** Initial DFT structural optimizations were carried out using the one-parameter hybrid meta-GGA functional TPSSh,[33] and split-valence basis sets including polarization functions for non-hydrogen atoms [SV(P)][34] were used for all light atoms. Small effective core potentials (ECPs)[35] were used for yttrium, lanthanum, and uranium as well as the larger triple-$\zeta$ basis sets with two sets of polarization functions (TZVP).[36] Large f-in-core pseudopotentials[37,38] and the corresponding quasi-relativistic basis sets of Dolg et al.[39] were used for cerium, which enforce the expected $f^1$ occupation of $Ce^{3+}$. Additional optimizations for all compounds were then performed using TZVP basis sets for all light atoms. The results at the TZVP level satisfactorily agree with experiment but differ from the SV(P) geometries in some cases. An additional optimization was performed on the cerium, lanthanum, and yttrium compounds using even larger QZVP basis sets for all atoms. During these structural optimizations, saddle points were frequently obtained. These structures had one small imaginary vibrational frequency corresponding to rotation of a $(C_5Me_5)^-$ ring. Only after tighter convergence criteria were used was a true minimum obtained, except for the cerium compound. The reported optimized structure for **Ce4** has one small imaginary vibrational mode, 4 cm$^{-1}$ in magnitude, corresponding to a spurious Cp-ring rotation. The overall difference in pertinent bond lengths between the metal and TMN group for TZVP and QZVP minima was negligible, but the positioning of the methyl groups relative to one another varied. The calculations performed for this work therefore represent local potential minima of these compounds that have characteristic Ln−TMN interactions and differ from the global potential energy minima only in the orientation and location of the methyl groups on the $\beta$-carbon atoms of the TMN rings. This behavior is not unexpected because of the crowded environment generated by bulky ligands in close proximity.

The TZVP values are referenced from here on, unless otherwise specified. Vibrational frequencies[40] were computed at the TZVP level, and all reported structures were confirmed to be minima by the absence of imaginary vibrational frequencies. The reported vibrational frequencies have been scaled by 0.95 to account for anharmonicities. Fine quadrature grids (at least size m4)[41] and $C_1$ symmetry were used throughout.

## ■ RESULTS

**Synthesis.** Reaction of KTMN with the metallocene tetraphenylborate complexes, $[(C_5Me_5)_2M][(\mu\text{-}Ph)_2BPh_2]$ (M = Y, Sm, Ce, U), occurs readily over the course of several hours in benzene to provide the TMN complexes $(C_5Me_5)_2M(TMN)$ in 55−84% yield, eq 1, despite the fact that KTMN is not soluble

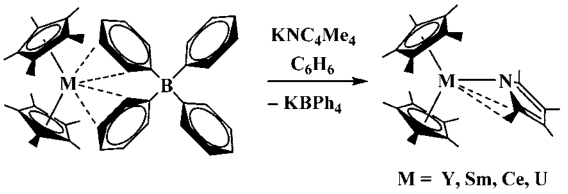

(1)

Table 2. X-ray Crystallographic Data and DFT Calculations on Y1/Y2, Sm3, Sm-P,Ce4, and U5/U6[a]

| | compound | | | | | | |
|---|---|---|---|---|---|---|---|
| | Y1a | Y1b | Y2 | Y-DFT | Sm3a | Sm3b | Sm-P |
| six-coordinate ionic radii (Å) | 0.90 | 0.90 | 0.90 | 0.90 | 0.958 | 0.958 | 0.958 |
| M−Cp* centroid (Å) | 2.341 | 2.347 | 2.344 | 2.375 | 2.410 | 2.419 | 2.439 |
| M−Cp* centroid (Å) | 2.342 | 2.338 | 2.342 | 2.374 | 2.414 | 2.406 | 2.400 |
| M−E (Å) | 2.263(2) | 2.282(2) | 2.266(2) | 2.295 | 2.320(3) | 2.337(3) | 2.892(2) |
| Cp* centroid−M−Cp* centroid (deg) | 139.4 | 138.6 | 139.4 | 139.8 | 139.1 | 138.2 | 136.21 |
| M−(E)−TMN centroid (deg) | 155.4 | 152.9 | 167.3 | 154.32 | 155.0 | 152.2 | 107.6 |
| M−(E)−C$^a$ (deg) | 105.6(1) | 106.5(1) | 115.7(2) | 106 | 105.4(3) | 106.3(3) | 75.1(2) |
| M−(E)−C$^d$ (deg) | 145.8(1) | 142.3(1) | 138.1(2) | 144 | 145.5(3) | 142.1(3) | 131.1(2) |
| M−C$^a$ (Å) | 2.959(2) | 2.986(2) | 3.125(2) | 2.991 | 3.003(4) | 3.035(4) | 3.021 |
| M−C$^e$H$_3$ (Å) | 2.938(2) | 3.024(2) | 3.198(4) | 2.992 | 2.968(4) | 3.058(4) | 3.033 |

| | compound | | | | | |
|---|---|---|---|---|---|---|
| | Ce4 | Ce DFT | U5a | U6a | U-DFT | La-DFT |
| six-coordinate ionic radii (Å) | 1.01 | 1.01 | 1.025 | 1.025 | 1.025 | 1.032 |
| M−Cp* centroid (Å) | 2.490 | 2.537 | 2.465 | 2.471 | 2.469 | 2.565 |
| M−Cp* centroid (Å) | 2.492 | 2.540 | 2.473 | 2.461 | 2.465 | 2.570 |
| M−E (Å) | 2.400(2) | 2.424 | 2.368(3) | 2.361(3) | 2.374 | 2.462 |
| Cp* centroid−M−Cp* centroid (deg) | 137.7 | 138.6 | 138.5 | 138.7 | 136.71 | 138.72 |
| M−(E)−TMN centroid (deg) | 153.9 | 158.14 | 156.8 | 157.3 | 153.43 | 147.71 |
| M−(E)−C$^a$ (deg) | 107.8(1) | 105.8 | 107.5(2) | 107.9(2) | 102 | 103 |
| M−(E)−C$^d$ (deg) | 141.2(2) | 147.2 | 144.3(2) | 143.2(2) | 149 | 142 |
| M−C$^a$ (Å) | 3.119(2) | 3.105 | 3.088(3) | 3.080(3) | 2.999 | 3.085 |
| M−C$^e$H$_3$ (Å) | 3.113(2) | 3.003 | 3.039(3) | 3.047(3) | 2.888 | 3.053 |

[a] E = N, P. C$^a$, C$^d$, and C$^e$ are defined in Figure 2.

in benzene. Similar results have been obtained in reactions of the $[(C_5Me_5)_2M][(\mu\text{-Ph})_2BPh_2]$ (M = Ln, U) salts with other alkali-metal reagents of low solubility.[8,20−27]

The $^1$H NMR spectrum of the diamagnetic yttrium complex **YA**contains resonances in a 30:6:6 ratio, which indicates that the TMN ligand in solution at room temperature is not locked in the asymmetric environment observed in the solid state, as described below and shown in eq 1. The $^1$H NMR spectra of the samarium, cerium, and uranium analogues are similar except that the resonances are paramagnetically shifted. Low-temperature $^1$H NMR spectroscopic studies on **YA** and **U5** down to 195 K showed the same pattern; i.e., no evidence has been found for a static asymmetric structure in solution. The spectrum is consistent with a fast equilibrium between asymmetric structures.

**Structure.** X-ray crystallography revealed considerable structural variability in these $(C_5Me_5)_2M(TMN)$ complexes (Table 1). In the case of yttrium, two crystals isolated from the *same* recrystallization mother liquor in hexanes crystallized in different space groups, $P2_1/c$ (**Y1**) and $P2_1/n$ (**Y2**). The $P2_1/c$ structure had two different crystallographically independent molecules in the unit cell with significantly different structural parameters (**Y1a** and **Y1b**). Hence, three molecular yttrium structures will be discussed arising from a single recrystallization. The samarium complex, **Sm3**, also crystallized from hexanes in $P2_1/c$ with two crystallographically independent molecules per unit cell (**Sm3a** and **Sm3b**), but these are similar in structure. Only one set of molecular structural data was obtained with cerium (**Ce4**) in $P2_1/c$, but two similar solid-state forms of the uranium complex $(C_5Me_5)_2U(TMN)$ were obtained: **U5** from hexanes and **U6** from toluene. Both of these crystallized in $P\bar{1}$, but **U5** had four crystallographically independent molecules in the unit cell and **U6** had two independent molecules. Consequently, structural data on 12 crystallographically independent molecules were obtained in this study. Only significant variations will be discussed, and crystallographic and computational data on only eight structures are presented in Table 2: **Y1a**, **Y1b**, **Y2**, **Sm3a**, **Sm3b**, **Ce4**, **U5a**, and **U6a**, as well as the known phosphoryl complex of Nief et al., $(C_5Me_5)_2Sm(PC_4Me_4)$ (**Sm-P**).[19]

X-ray crystallography showed that in none of these eight cases does the TMN anion attach to the $[(C_5Me_5)_2M]^+$ metallocene unit as a simple $\eta^1$-nitrogen-donor atom ligand. In each case, as detailed below, TMN binds in a pseudo-$\eta^3$ manner, in which one $\alpha$-ring carbon and its attached methyl group, C(21) and C(25), respectively, are oriented toward the metal, as shown in Figure 1.

All of the compounds in this study are similar in the sense that the nitrogen-donor atom of the TMN ligand is in the plane that bisects the ($C_5Me_5$ centroid)−M−($C_5Me_5$ centroid) angle; i.e., it is equidistant from each $C_5Me_5$ ring centroid. However, the nitrogen donor is oriented to the side of the ($C_5Me_5$ centroid)−M−($C_5Me_5$ centroid) plane, such that the $\alpha$-ring carbon and its attached methyl group are oriented toward the metal. In each case, the M−N distance is in the single-bond range for that metal. For instance, the M−N(TMN) bond distances are 2.263(2), 2.320(3), and 2.368(3) Å for **Y1a**, **Sm3a**, and **U5**, respectively, compared to the $(C_5Me_5)_2M[N(SiMe_3)_2]$ M−N bond distances of 2.274(5),[42] 2.301,[43] and 2.352(2)[20] Å for M = Y, Sm, and U, respectively. In all of the complexes, the C$^a$−C$^b$ and C$^c$−C$^d$ distances (using the carbon labels of Figure 2) are ~0.04 Å shorter than C$^b$−C$^c$ (Table S2 in the Supporting Information). Similar shortening of C$^a$−C$^b$ and C$^c$−C$^d$ versus C$^b$−C$^c$ is found in $(CH_2C_6H_4NMe_2\text{-}o)_2Sc(\eta^1\text{-TMN})$.[11]

Each complex has one $\alpha$-ring carbon much closer to the metal than the other such that the M−N−C$^a$ angle is much smaller than the M−N−C$^d$ analogue (Figure 2A). These pairs of angles as well as the difference in each pair vary considerably from one structure to another even with crystals of the same

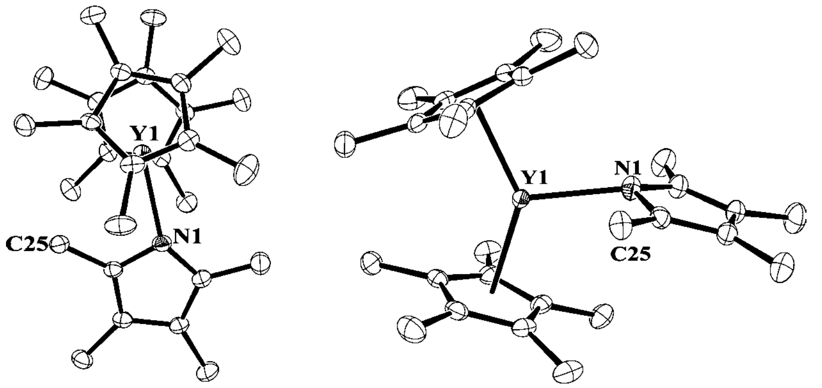

**Figure 1.** ORTEP diagrams of one crystallographically independent molecule (**Y1a**) of **Y1** drawn at the 50% probability level. Two perspectives are shown. Selected structural data can be found in Table 2. Hydrogen atoms are omitted for clarity.

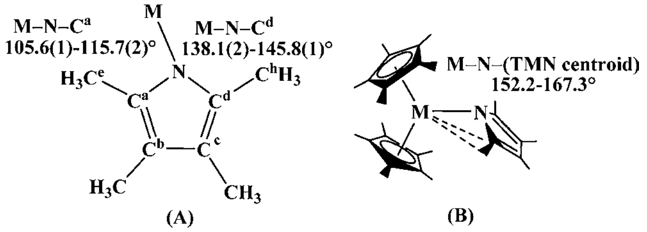

**Figure 2.** (A) Variation in the M–N–C$^a$ and M–N–C$^d$ angles and (B) variation in the M–N–(TMN centroid) angles (M = Y, Sm, Ce, U).

metal grown from the same mother liquor (Table 2). Another structural variation in this series that is detailed in Table 2 is the M–N–(TMN centroid) angles shown in Figure 2B.

The close approach of C$^a$ and C$^e$ found in the solid state is also predicted in DFT calculations. The pseudo-$\eta^3$ structure for the TMN ligand proved to be a minimum in the DFT calculations in every case studied regardless of the starting point for the calculation in terms of an $\eta^5$-, $\eta^3$-, or $\eta^1$-TMN ring. The specific data along with the DFT calculations are presented below for yttrium, samarium, cerium, and uranium.

**Structural Comparisons for Y1a, Y1b, and Y2.** DFT calculations using the yttrium complex **Y1** as a starting point provided Y–($C_5Me_5$ centroid), Y–N(TMN), and ($C_5Me_5$ centroid)–Y–($C_5Me_5$ centroid) values that are very close to those found in **Y1a**, **Y1b**, and **Y2**, as shown in Table 2. The calculated distances are within 0.04 Å and the angles are within 4° of the experimental values, which are similar in the three yttrium variants. The ($C_5Me_5$ centroid)–M–($C_5Me_5$ centroid) angles in all of the complexes in this study are similar and will not be discussed further.

The DFT calculations predict that the $\alpha$-ring carbon and the associated methyl group will be tipped toward the yttrium. The amount of distortion can be gauged by the difference in the two M–N–C(alpha ring) angles in each structure. These are calculated to be 106° and 144° for M–N–C$^a$ and M–N–C$^d$ in $(C_5Me_5)_2Y(TMN)$, respectively. These angles are very close to the experimental values in **Y1a** [105.6(1)° and 145.8(1)°] and **Y1b** [106.5(1)° and 142.3(1)°]. The calculations also predict a 154° Y–N–(TMN centroid) angle close to the 155.36° and 152.92° values for **Y1a** and **Y1b**, respectively. The calculated Y–C$^a$ distance is 2.99 Å, and the carbon of the methyl attached to C$^a$, labeled C$^e$, is also predicted to be 2.99 Å from yttrium. The similarity of these calculated distances for C$^a$ and C$^e$ agrees with the similarity of the values in **Y1a** [2.959(2) and 2.938(2) Å] and **Y1b** [2.986(2) and 3.024(2) Å]. This is an exceptionally good match and shows another example of the power of DFT to predict weak interactions in these types of complexes.[44,45] These distances also compare well with the experimentally observed 2.970 Å Y–C(SiMe$_3$) distance in $(C_5Me_5)_2Y[N(SiMe_3)_2]$.[42] The related compound, $(C_5Me_5)_2Y(C_5Me_4H)$, also showed this pseudo-$\eta^3$ interaction, but the Y–C$^a$ distance and Y–C–($C_5Me_4H$ centroid) angle are smaller at 2.879 Å and 113.33°, respectively.[8]

Although the calculations for the Y–C$^a$ and Y–C$^e$ distances are very close to the actual distances in **Y1b**, the distances in **Y1a** are 0.03–0.08 Å shorter than those in **Y1b**. Because there are two different sets of experimental values, the calculation cannot match both. Because the crystal structure of the third yttrium variant, **Y2**, differs significantly from those of **Y1a** and **Y1b** in these parameters, there is an even greater discrepancy from the calculations. The Y–N–C$^a$/Y–N–C$^d$ angle disparity is smaller for **Y2**: 115.7(2)° and 138.1(2)°. The less acute Y–N–C$^a$ angle leads to longer Y–C distances for the C$^a$ and C$^e$: 3.125(2) Å for Y–C$^a$ and 3.198(4) Å for Y–C$^e$ compared to all analogous distances in **Y1** that are less than 3 Å.

The 167.3° experimental Y–N–(TMN centroid) angle in **Y2** is also much larger than those in **Y1**, as shown in the overlaid structures of **Y2** and **Y1b** in Figure 3. In fact, the 167.3° angle

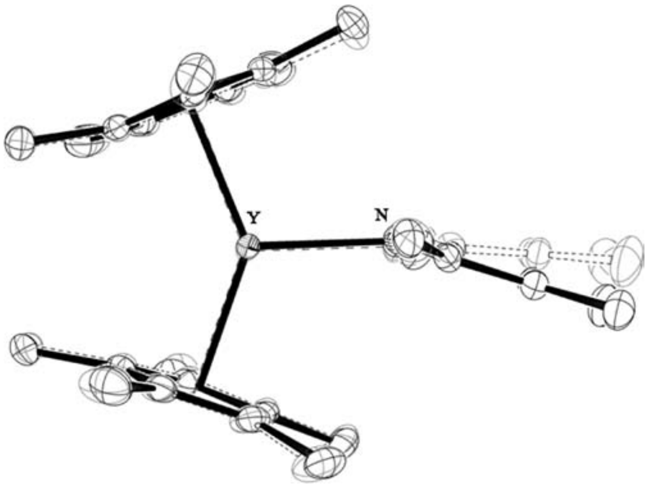

**Figure 3.** Side views of **Y1b** and **Y2** overlaid to show the difference in the M–N–(TMN centroid) angle between two crystals grown from the same mother liquor.

in **Y2** is the largest Y−N−(TMN centroid) angle found in any of the structures. In all of the other calculations and experimental data, these angles fall in the range 147.56−157.3°.

**Structures of the 4f Complexes: Sm3a, Sm3b, Sm-P, and Ce4.** The samarium and cerium complexes **Sm3** and **Ce4** crystallize in the same space group as **Y1**, $P2_1/c$, rather than the $P2_1/n$ of **Y2**. The crystal structures of the two samarium variants, **Sm3a** and **Sm3b**, and the cerium analogue **Ce4** have M−($C_5Me_5$ centroid) and M−N distances that are longer than those in **Y1a**, **Y1b**, and **Y2**, as expected based on the larger radial sizes of samarium and cerium (Table 2). The metrical parameters for the C$^a$ and C$^e$ interactions in **Sm3a**, **Sm3b**, and **Ce4** match most closely with those of **Y1** and not **Y2**. Hence, the 105.4(3)−107.8(1)° M−N−C$^a$ and 141.2(2)−145.5(3)° M−N−C$^d$ values have a larger difference than the 115.7(2)° and 138.1(2)° analogues in **Y2**. The M−C$^a$ and M−C$^e$ distances in **Sm3a**, **Sm3b**, and **Ce4** are also similar, whereas they are rather different in **Y2** (0.07 Å difference). Comparing the **Sm3** and **Sm-P** structures[19] shows that while the Sm−P bond is 0.53 Å longer than the Sm−N bonds, the Sm−C$^a$/C$^e$ distances are the same within error. DFT studies on the samarium complex were not attempted to mimimize the number of open-shell calculations, but studies for cerium and lanthanum did converge and are discussed below.

The DFT calculations done with lanthanum and cerium give similar predictions; the differences are mainly consistent with the different radial sizes of the ions. The lanthanum and cerium calculations are also similar to the yttrium calculation in terms of angles. Because the yttrium calculations match **Y1** and because **Ce4**, **Sm3a**, and **Sm3b** are experimentally similar to **Y1**, the lanthanum and cerium calculations are good predictors for the angles of the cerium and samarium complexes. However, the distances in the lanthanum and cerium calculations differ from those of the yttrium calculation even considering the difference in ionic radii. For example, the 2.54 Å calculated Ce−($C_5Me_5$ centroid) distances are about 0.2 Å larger than the 2.34 Å calculated yttrium analogues, while the calculated 3.105 Å Ce−C$^a$ distance is only 0.11 Å larger than the 2.991 Å yttrium analogue and the 3.003 Å Ce−C$^e$ distance is nearly equal to the 2.992 Å yttrium analogue. This suggests more C$^a$ and C$^e$ interaction for cerium relative to yttrium, which is surprising given the higher charge to radius ratio of yttrium. The 3.113(2) Å Ce−C$^e$ experimental value is much larger than the calculated cerium value and matches better with the yttrium experimental values when the 0.101 Å difference in the ionic radii is considered. While the differences in cerium calculated and experimental are larger than those for **Y1a** and **Y1b**, the error is no larger than 5% in the bond lengths, which is within the error limit of DFT.

**4f versus 5f Structures: Cerium versus U5 and U6.** Because U$^{3+}$ is similar in size to Ce$^{3+}$,[28] the structures provide an opportunity for a lanthanide versus actinide comparison. There are four crystallographically independent molecules in **U5** and two in **U6**, but these are all similar within error, and so only one, **U5**, will be described. The angles in **Ce4** and **U5** are all quite similar. The 2.490−2.492 Å Ce−($C_5Me_5$ centroid) distances are numerically larger than the 2.465−2.473 Å uranium analogues even though uranium is slightly larger, but these numbers are very similar with the error limits. The 3.119(2) Å Ce−C$^a$ and 3.113(2) Å Ce−C$^e$ distances are both longer than the 3.088(3) and 3.039(3) Å uranium analogues. Hence, the uranium complex shows relatively more interaction with C$^a$ and C$^e$. The DFT calculations also predict a stronger C$^a$ and C$^e$ interaction for uranium compared to cerium, as is observed experimentally.

Overall, there is quite good agreement between the calculated and experimental data in predicting the C$^a$ and C$^e$ interactions, except for **Y2**, which is structurally different from **Y1a** and **Y1b**. For comparison, the calculations for $(C_5Me_5)_2Y[N(SiMe_3)_2]$, which has an asymmetric structure with a silylmethyl group oriented toward yttrium, were also examined. The results matched quite closely to the experimental values (Table S1 in the Supporting Information).

**IR Spectroscopy.** DFT calculations also predict that these complexes will have some IR absorbances at lower wavenumbers than typical C−H bonds, as might be expected due to the close approach of the C$^e$ methyl group. The experimentally found absorbances matched in both energy and intensity within the expected ±5% error of DFT calculations. The calculated/found values in cm$^{-1}$ are as follows: Y, 2689/2724; Ce, 2745/2730; U, 2710/2722.

## DISCUSSION

Bis(pentamethylcyclopentadienyl) metal tetramethylpyrrolyl complexes, $(C_5Me_5)_2M(NC_4Me_4)$, can be readily made from the tetraphenylborate salts $[(C_5Me_5)_2M][(\mu\text{-Ph})_2BPh_2]$ and $KNC_4Me_4$ and fully characterized including X-ray diffraction. Although the solid-state structures of these complexes approximate the putative $(\eta^5\text{-}C_5Me_5)_2M(\eta^1\text{-}C_5Me_5)$ intermediate that was targeted in this study, extra coordination of one side of the TMN ring to the metal is observed in each case. This behavior echoes that of $(C_5Me_5)_2M(C_5Me_4H)$ (M = Y, Lu),[8] where an even stronger interaction was observed. Additional metal−ligand interactions are not unusual for large Lewis acidic metals,[19,42,44,45] and it seems possible for an $(\eta^1\text{-}C_5Me_5)^-$ ligand to display the same behavior as the TMN and $(C_5Me_4H)^-$ ligands.

Additional metal−ligand interactions in the rare-earth metallocenes are well-known, as exemplified by complexes such as $(C_5Me_5)_2Y[N(SiMe_3)_2]$[42] and $(C_5Me_5)_2Ln[CH(SiMe_3)_2]$ (Ln = Y,[42] Nd,[46] Ce[47]). In each case, a methyl group of a silyl ligand is oriented toward the metal center. Strangely, the uranium homologue, $(C_5Me_5)_2U[N(SiMe_3)_2]$, does not show such interactions.[20] It is not clear why the smaller metal, yttrium, would show such interactions with both $[N(SiMe_3)_2]^-$ and TMN, while uranium has these interactions only with TMN.

Comparisons can also be made with Nief's phosphorus analogue,[19] **Sm-P**. Even in the presence of the larger phosphorus atom with a 2.892(2) Å Sm−P bond, much longer than the 2.320(3)−2.337(3) Å Sm−N distances in **Sm3**, the phosphoryl ring simply bends even more to achieve electronic and steric saturation of the metal center via the additional metal−ligand interaction. The fact that the Sm−C$^a$ and Sm−C$^e$ distances in both **Sm3** and **Sm-P** are identical suggests that the degree of bending of the M−E−C$^a$ (E = P, N) angle is not energetically significant to the solid-state structure because the structure is dominated by the $\alpha$-methyl group interaction.

One of the most significant features of the $(C_5Me_5)_2M(NC_4Me_4)$ structures is that numerous variations are energetically accessible in the solid state. The isolation of two $(C_5Me_5)_2Y(NC_4Me_4)$ crystals from the same mother liquor with significantly different metal-to-TMN binding and the fact that one of these crystals had two different crystallographically independent molecules in the unit cell demonstrate how easy it is to get different solid-state structures from this particular ligand set. A total of 12 different crystallographically independent molecules were identified with just four metals. Clearly, there are several energetically acceptable orientations of the 14 methyl groups on these 3 ligands around the large ionic metals.

This structural variability was also detected in the DFT studies. Saddle points in the calculations were identified that indicated the presence of several energetically similar structures. More stringent conditions had to be imposed to identify minima, and these must be regarded as local rather than global minima. This is consistent with the experimental data because variation in the structure of, for example, $(C_5Me_5)_2Y(NC_4Me_4)$ could not be modeled by one calculated structure.

This study demonstrates how easy it can be to overinterpret bond distances and angles from a single-crystal structure. The isomers **Y1** and **Y2** were grown simultaneously in the same vial and only differed in which crystal was picked out of dozens of crystals, yet they show large deviations in structure. Small differences in the crystallization methods can have significant effects on the bond distances and angles with compounds that have shallow potential energy minima as found here.

It remains to be determined if the structural variability observed here is general or if this is a peculiar aspect of the TMN ligand. Few data are available on this point.[48] Generally, in molecular chemistry (but not solid state chemistry), once one good crystal structure is obtained, it is assumed that this is "the structure" of the complex and no further attempts are made to get crystals in different space groups from different solvents, etc.

## ■ CONCLUSION

The combination of a TMN ligand with two pentamethylcyclopentadienyl ligands generates a ligand set that shows unusually large variations in structure when attached to rare-earth metal and uranium ions. The TMN ligand in these $(C_5Me_5)_2M(NC_4Me_4)$ complexes binds not only through the nitrogen but also through interactions with an adjacent carbon and its attached methyl group. Crystallographic data on complexes of yttrium, samarium, cerium, and uranium show that the structural details of the additional binding are highly variable in this environment of three polyalkyl rings with these large Lewis acidic metals. DFT calculations support the structural observations in showing that these additional interactions can be predicted and the potential energy surface is shallow for this type of complex.

## ■ ASSOCIATED CONTENT

### Ⓢ Supporting Information

X-ray crystallographic data of compounds **Y1−U6** (CCDC 879699−879704) in CIF format, X-ray data collection, structure solution, and refinement. This material is available free of charge via the Internet at http://pubs.acs.org.

## ■ AUTHOR INFORMATION

### Corresponding Author

*E-mail: wevans@uci.edu.

### Notes

The authors declare no competing financial interest.

## ■ ACKNOWLEDGMENTS

We thank the Chemical Sciences, Geosciences, and Biosciences Division of the Office of Basic Energy Sciences of the Department of Energy through Grant DE-FG02-10ER16161 (to W.J.E.) for supporting the experimental studies and the U.S. National Science Foundation through Grant CHE-0840513 for supporting the theoretical studies, Thomas J. Mueller for preliminary experiments, and Ryan Zarkesh for assistance with X-ray crystallography.

## ■ REFERENCES

(1) Evans, W. J.; Davis, B. L. *Chem. Rev.* **2002**, *102*, 2119.

(2) Evans, W. J.; Rego, D. B.; Ziller, J. W.; DiPasquale, A. G.; Rheingold, A. L. *Organometallics* **2007**, *26*, 4737.

(3) Evans, W. J.; Kozimor, S. A.; Nyce, G. W.; Ziller, J. W. *J. Am. Chem. Soc.* **2003**, *125*, 13831.

(4) Evans, W. J.; Kozimor, S. A.; Ziller, J. W. *Organometallics* **2005**, *24*, 3407.

(5) Evans, W. J.; Nyce, G. W.; Johnston, M. A.; Ziller, J. W. *J. Am. Chem. Soc.* **2000**, *122*, 12019.

(6) Evans, W. J.; Kozimor, S. A.; Ziller, J. W. *J. Am. Chem. Soc.* **2003**, *125*, 14264.

(7) Evans, W. J.; Mueller, T. J.; Ziller, J. W. *J. Am. Chem. Soc.* **2009**, *131*, 2678.

(8) Demir, S.; Mueller, T. J.; Ziller, J. W.; Evans, W. J. *Angew. Chem., Int. Ed.* **2011**, *123*, 535.

(9) Marks, T. J.; Kolb, J. R. *J. Organomet. Chem.* **1974**, *82*, C35.

(10) Schumann, H.; Lee, P. R.; Dietrich, A. *Chem. Ber.* **1990**, *123*, 1331.

(11) Nishiura, M.; Mashiko, T.; Hou, Z. *Chem. Commun.* **2008**, 2019.

(12) Bérubé, C. D.; Gambarotta, S.; Yap, G. P. A.; Cozzi, P. G. *Organometallics* **2003**, *22*, 434.

(13) Yang, Y.; Li, S.; Cui, D.; Chen, X.; Jing, X. *Organometallics* **2006**, *26*, 671.

(14) Yang, Y.; Liu, B.; Lv, K.; Gao, W.; Cui, D.; Chen, X.; Jing, X. *Organometallics* **2007**, *26*, 4575.

(15) Xiang, L.; Wang, Q.; Song, H.; Zi, G. *Organometallics* **2007**, *26*, 5323.

(16) Wang, Q.; Xiang, L.; Song, H.; Zi, G. *Inorg. Chem.* **2008**, *47*, 4319.

(17) Zi, G.; Xiang, L.; Song, H. *Organometallics* **2008**, *27*, 1242.

(18) Cui, C.; Shafir, A.; Reeder, C. L.; Arnold, J. *Organometallics* **2003**, *22*, 3357.

(19) Nief, F.; Ricard, L. *Organometallics* **2001**, *20*, 3884.

(20) Evans, W. J.; Nyce, G. W.; Forrestal, K. J.; Ziller, J. W. *Organometallics* **2002**, *21*, 1050.

(21) Evans, W. J.; Perotti, J. M.; Ziller, J. W. *J. Am. Chem. Soc.* **2005**, *127*, 3894.

(22) Evans, W. J.; Lee, D. S.; Johnston, M. A.; Ziller, J. W. *Organometallics* **2005**, *24*, 6393.

(23) Evans, W. J.; Lee, D. S.; Lie, C.; Ziller, J. W. *Angew. Chem., Int. Ed.* **2004**, *43*, 5517.

(24) Evans, W. J.; Mueller, T. J.; Ziller, J. W. *Chem.—Eur. J.* **2010**, *16*, 964.

(25) Mueller, T. J.; Nyce, G. W.; Evans, W. J. *Organometallics* **2011**, *30*, 1231.

(26) MacDonald, M. R.; Ziller, J. W.; Evans, W. J. *Inorg. Chem.* **2011**, *50*, 4092.

(27) Evans, W. J.; Kozimor, S. A.; Ziller, J. W. *Science* **2005**, *309*, 1835.

(28) Shannon, R. *Acta Crystallogr.* **1976**, *A 32*, 751.

(29) Evans, W. J.; Davis, B. L.; Champagne, T. M.; Ziller, J. W. *Proc. Natl. Acad. Sci. U.S.A.* **2006**, *103*, 12678.

(30) Evans, W. J.; Seibel, C. A.; Ziller, J. W. *J. Am. Chem. Soc.* **1998**, *120*, 6745.

(31) Evans, W. J.; Perotti, J. M.; Kozimor, S. A.; Champagne, T. M.; Davis, B. L.; Nyce, G. W.; Fujimoto, C. H.; Clark, R. D.; Johnston, M. A.; Ziller, J. W. *Organometallics* **2005**, *24*, 3916.

(32) Chase, K. J.; Grimes, R. N. *Organometallics* **1989**, *8*, 2492.

(33) Staroverov, V. N.; Scuseria, G. E.; Tao, J.; Perdew, J. P. *J. Chem. Phys.* **2003**, *119*, 12129.

(34) Schäfer, A.; Horn, H.; Ahlrichs, R. *J. Chem. Phys.* **1992**, *97*, 2571.

(35) Andrae, D. H. U.; Dolg, M. *Theor. Chim. Acta* **1990**, *77*, 123.

(36) Weigend, F.; Ahlrichs, R. *Phys. Chem. Chem. Phys.* **2005**, *18*, 3297.
(37) Dolg, M.; Stoll, H.; Preuss, H. *Theor. Chim. Acta* **1993**, *85*, 441.
(38) Yang, J.; Dolg, M. *Theor. Chem. Acc.* **2005**, *113*, 212.
(39) Dolg, M.; Stoll, H.; Savin, A.; Preuss, H. *Theor. Chim. Acta* **1989**, *75*, 173.
(40) Deglmann, P.; Furche, F.; Ahlrichs, R. *Chem. Phys. Lett.* **2002**, *362*, 511.
(41) Treutler, O.; Ahlrichs, R. *J. Chem. Phys.* **1995**, *102*, 346.
(42) Den Haan, K. H.; De Boer, J. L.; Teuben, J. H.; Spek, A. L.; Kojic-Prodic, B.; Hays, G. R.; Huis, R. *Organometallics* **1986**, *5*, 1726.
(43) Evans, W. J.; Keyer, R. A.; Ziller, J. W. *Organometallics* **1993**, *12*, 2618.
(44) Perrin, L.; Maron, L.; Eisenstein, O.; Lappert, M. F. *New J. Chem.* **2003**, *27*, 121.
(45) Jaffart, J.; Etienne, M.; Maseras, F.; McGrady, J. E.; Eisenstein, O. *J. Am. Chem. Soc.* **2001**, *123*, 6000.
(46) Jeske, G.; Lauke, H.; Mauermann, H.; Swepston, P. N.; Schumann, H.; Marks, T. J. *J. Am. Chem. Soc.* **1985**, *107*, 8091.
(47) Heeres, H. J.; Renkema, J.; Booij, M.; Meetsma, A.; Teuben, J. H. *Organometallics* **1988**, *7*, 2495.
(48) Minasian, S. G.; Krinsky, J. L.; Arnold, J. *Chem. Eur. J.* **2011**, *17*, 12234.